Post-translational Regulation of DNA Polymerase η, a Connection to Damage-Induced Cohesion in *Saccharomyces cerevisiae*

Pei-Shang Wu,* Elin Enervald,*,[1] Angelica Joelsson,* Carina Palmberg,[†] Dorothea Rutishauser,[†,2] B. Martin Hällberg,* and Lena Ström*,[3]

*Department of Cell and Molecular Biology and [†]Department of Medical Biochemistry and Biophysics, Karolinska Institutet, Stockholm SE-171 77, Sweden

ORCID IDs: 0000-0003-2303-103X (D.R.); 0000-0002-8898-3675 (L.S.)

ABSTRACT Double-strand breaks that are induced postreplication trigger establishment of damage-induced cohesion in *Saccharomyces cerevisiae*, locally at the break site and genome-wide on undamaged chromosomes. The translesion synthesis polymerase, polymerase η, is required for generation of damage-induced cohesion genome-wide. However, its precise role and regulation in this process is unclear. Here, we investigated the possibility that the cyclin-dependent kinase Cdc28 and the acetyltransferase Eco1 modulate polymerase η activity. Through *in vitro* phosphorylation and structure modeling, we showed that polymerase η is an attractive substrate for Cdc28. Mutation of the putative Cdc28-phosphorylation site Ser14 to Ala not only affected polymerase η protein level, but also prevented generation of damage-induced cohesion *in vivo*. We also demonstrated that Eco1 acetylated polymerase η *in vitro*. Certain nonacetylatable polymerase η mutants showed reduced protein level, deficient nuclear accumulation, and increased ultraviolet irradiation sensitivity. In addition, we found that both Eco1 and subunits of the cohesin network are required for cell survival after ultraviolet irradiation. Our findings support functionally important Cdc28-mediated phosphorylation, as well as post-translational modifications of multiple lysine residues that modulate polymerase η activity, and provide new insights into understanding the regulation of polymerase η for damage-induced cohesion.

KEYWORDS polymerase eta; cohesin; damage-induced cohesion; Cdc28/Cdk1; Eco1

DNA double-strand breaks (DSBs) can potentially be deleterious to cells since inefficiently repaired DSBs affect the physical integrity of chromosomes, and thereby genome stability. As part of the DSB response, cohesins are recruited to the break site (Kim *et al.* 2002; Ström *et al.* 2004; Unal *et al.* 2004), and *de novo* cohesion established locally at the DSB. This so-called DSB proximal damage-induced cohesion is instrumental for accurate DSB repair. We previously demonstrated that damage-induced cohesion, established genome-wide on undamaged chromosomes in *Saccharomyces cerevisiae* (Ström *et al.* 2004, 2007; Unal *et al.* 2007), depends on polymerase eta (Polη) (Enervald *et al.* 2013). However, our knowledge on its regulation during this process remained sparse.

Polη (encoded by the *RAD30* gene) is one of three known translesion synthesis (TLS) polymerases in *S. cerevisiae* and belongs to the Y-family of specialized DNA polymerases. TLS polymerases are characterized by an open active site, thereby having the capacity to catalyze nucleotide incorporation opposite bulky lesions that cannot be bypassed by high-fidelity replicative DNA polymerases (Waters *et al.* 2009). Polη is mainly known for incorporation of two adenine bases opposite cyclobutane pyrimidine dimers, the major type of DNA lesions induced by ultraviolet (UV) irradiation, in a principally error-free manner (Johnson *et al.* 1999b). Accordingly, impaired Polη function leads to severe UV sensitivity, and is the cause of

doi: https://doi.org/10.1534/genetics.120.303494
Manuscript received June 9, 2020; accepted for publication October 6, 2020; published Early Online October 8, 2020.
Available freely online through the author-supported open access option.
Supplemental material available at figshare: https://doi.org/10.25386/genetics.13055816.
[1]Present address: Department of Molecular Biosciences, The Wenner-Gren Institute, Stockholm University, Stockholm SE-106 91, Sweden.
[2]Present address: Institute of Pathology and Molecular Pathology, University Hospital Zurich, Zurich 8091, Switzerland.
[3]Corresponding author: Karolinska Institutet, Department of Cell and Molecular Biology, Biomedicum 7B, B07, SE-171 77 Stockholm, Sweden. E-mail: lena.strom@ki.se

xeroderma pigmentosum variant syndrome with high incidence of skin cancer (Johnson *et al.* 1999a; Masutani *et al.* 1999).

Besides its canonical TLS activity, growing evidence suggest Polη TLS-independent functions (Acharya *et al.* 2019), such as DNA single-strand gap-filling for immunoglobulin somatic hypermutation, and extension of D-loops during DSB repair via homologous recombination (HR). Polη also has noncatalytic functions, such as recruiting human E3 ubiquitin ligase RAD18 to PCNA (Durando *et al.* 2013), and being important for the mentioned damage-induced cohesion in yeast (Enervald *et al.* 2013). Involvement of Polη in these multiple processes implied various interaction partners for distinct functions, and potential regulation through differential post-translational modifications.

In line with this, Polη activity is strictly regulated, presumably to avoid potential misincorporation of nucleotides due to its low fidelity on undamaged templates. Polη ubiquitination, for example, restricts its accessibility to replication forks (Cipolla *et al.* 2019). In addition, phosphorylation of human Polη is required for its localization to sites of UV-induced DNA lesions (Chen *et al.* 2008; Bertoletti *et al.* 2017; Peddu *et al.* 2018). These findings prompted us to investigate whether Polη would be regulated through post-translational modification(s) also for formation of damage-induced cohesion.

Cohesin is a highly conserved, multisubunit protein complex composed of the structural maintenance of chromosome proteins Smc1 and Smc3, the kleisin subunit Scc1 (or Mcd1), and the HEAT repeat protein Scc3. Two additional HEAT repeat proteins, Pds5 and Wpl1, are associated with the complex at substochiometric levels (Nasmyth and Haering 2009). Cohesin complexes are loaded on DNA before replication onset through the action of the cohesin loader Scc2-Scc4 (Ciosk *et al.* 2000). The canonical function of cohesin is to generate sister chromatid cohesion during S phase, which is maintained until anaphase (Nasmyth and Haering 2009; Peters and Nishiyama 2012; Uhlmann 2016). Eco1 is the acetyltransferase that determines establishment of sister chromatid cohesion via acetylation of the Smc3 subunit (Rolef Ben-Shahar *et al.* 2008; Unal *et al.* 2008; Zhang *et al.* 2008), which has been suggested to counteract a cohesion antiestablishment activity performed by Wpl1 together with Pds5 and Scc3 (Gerlich *et al.* 2006; Chan *et al.* 2012; Lopez-Serra *et al.* 2013). Interestingly, Eco1 is targeted for degradation at the end of S phase through interdependent actions of the Cdc28, Cdc7, and Mck1 kinases. However, Cdc7 is inactivated in response to DSBs. Consequently, Eco1 is stabilized, thereby enabling formation of damage-induced cohesion even postreplication (Lyons *et al.* 2013). We previously reported that overexpression of Eco1 rescues the lack of damage-induced cohesion in Polη-deficient cells (Enervald *et al.* 2013). Therefore, we speculated that Eco1-mediated acetylation regulates Polη for their concerted action during establishment of damage-induced cohesion.

Since Polη protein level is regulated in a cell-cycle-dependent manner (Plachta *et al.* 2015; Bertoletti *et al.* 2017), Cdc28 appeared to be another potential regulator of Polη. Cdc28, also known as Cdk1, is the sole cyclin-dependent kinase (CDK) in *S. cerevisiae*. The temporal regulation of Cdc28 is controlled by association with cell cycle phase-specific cyclins. Thus, Cdc28 is largely inactive in G_1 due to low levels of cyclins, while it is active from late G_1 until anaphase. Cdc28/cyclin complexes regulate cell cycle progression through phosphorylation of targets involved in cellular processes, such as cell cycle checkpoints (Morgan 1997; Enserink and Kolodner 2010). Besides its essential role for cell cycle regulation, Cdc28 is important for DNA damage checkpoint activation and for DSB repair via HR (Ira *et al.* 2004). Cdc28 also genetically interacts with Eco1 and Scc1 (Heo *et al.* 1999; Brands and Skibbens 2008), besides regulating Eco1 stability, as described above.

Here we aimed at improving our understanding of Polη regulation for damage-induced cohesion genome-wide. We investigated the possibilities that Cdc28 and Eco1 act as modifiers of Polη *in vitro*, and examined the functional importance of identified modifications *in vivo*. Through *in vitro* phosphorylation and structure modeling, we showed that Polη is an attractive substrate for Cdc28. We also found that putative Cdc28 mediated Polη-S14 phosphorylation affects Polη protein level, and is important for generation of damage-induced cohesion *in vivo*. In addition, we demonstrated that Eco1 acetylated Polη *in vitro*. Furthermore, Eco1 is required for cell survival after UV irradiation but acts in parallel with Polη. Several nonacetylatable Polη mutants showed reduced protein level, deficient nuclear accumulation, and affected the TLS activity of Polη. Taken together, our findings show that Cdc28-mediated phosphorylation and post-translational modifications of lysines modulate Polη activity. Identification of Cdc28 as a potential regulator also provides new insight into understanding the regulation of Polη for damage-induced cohesion.

Materials and Methods

Yeast strains and growth conditions

All *S. cerevisiae* yeast strains were W303 derivatives (*ade2-1 trp1-1 can1-100 leu2-3, 112 his3-11, 15 ura3-1 RAD5 GAL psi*$^+$). Most strains were haploids, and a few diploids (listed in Supplemental Material, Table S1). Gene deletions were performed with one-step replacement, using the kanamycin (*kanMX6*)-, the hygromycin (*hphMX4*)-, or the nourseothricin (*natMX4*)-resistance marker. Transformations were performed with the lithium acetate method. Some strains were crossed to obtain desired genotypes. Yeast extract peptone (YEP) supplemented with 40 μg/ml adenine was used as yeast media.

Mutagenesis and plasmids

To generate Polη single-point mutants, the full-length *RAD30* ORF was amplified from genomic DNA with primers where the 5′ ends were flanked with recognition sequences for the restriction enzymes HindIII and SalI. The amplified product

was then cloned into HindIII- and SalI-digested pAG25 (*natMX4* marked) or pAG32 (*hphMX4* marked) plasmids (Euroscarf). The cloned *RAD30-natMX4* or *RAD30-hphMX4* vector was used as template for PCR amplifications with Phusion high-fidelity DNA polymerase. Designed forward primers including desired point mutation annealed to the *RAD30* internal sequence; while the reverse primer, with *RAD30* downstream overhang, annealed after the plasmid selection marker. Amplified PCR fragments were transformed, and NAT^+ or HPH^+ candidates were analyzed with PCR to confirm correct integrations. Point mutations were verified by DNA sequencing (Toulmay and Schneiter 2006).

To generate Polη "*in vivo*" and "*in vitro*" multiple KR mutants, we designed *RAD30* alleles containing selected multiple-point mutations with additions of HindIII and SalI recognition sequences at the 5′ and 3′ ends. Designed sequences together with the pAG32 vector were sent to Invitrogen GeneArt Gene synthesis (Thermo Fisher Scientific) for gene synthesis and subsequent cloning according to our design. These plasmids were used as PCR template. A forward primer, with *RAD30* upstream overhang, was designed to anneal 14 bp away from the *RAD30* start codon; and a reverse primer, with *RAD30* downstream overhang, annealed to the plasmid after the *hphMX4* cassette. Selection of candidates from transformations was performed as above.

Spot assay

Yeast cells cultured in YEPD (glucose, final 2%) were grown to midlog phase. Twenty thousand cells were pelleted according to OD_{600}, resuspended in water and 10-fold serially diluted before spotting on assigned plates. Spotted cells were then exposed to indicated doses of ultraviolet C (UVC; 254 nm) and kept dark for 3 days at room temperature, or 2 days at 30° or 32°. Two technical repeats were included for each treatment and each spot assay was done at least twice.

Damage-induced cohesion assay

Cells harboring the *smc1* temperature-sensitive (*ts*) allele (*smc1-259*) were grown to exponential phase at 23° in YEPR (raffinose, final 2%). Subsequently benomyl (final 80 μg/ml) was added for G_2/M phase arrest. Galactose (final 2%) was then added for 1 hr to induce expression of the ectopic P_{GAL}-*SMC1-MYC*, and P_{GAL}-*HO* to generate DSBs at the *MAT* locus on chromosome III. In response to break induction, both endogenous and ectopic Smc1 are used for damage-induced cohesion. Cohesion established during replication depends on the *smc1-259 ts* allele alone, and was inactivated by raising the temperature to 35°. The break induction was stopped by switching the media to YEPD with benomyl, and samples were collected up to 90 min at 35°. Collected samples were fixed for 15 min with 3.7% formaldehyde at 23°, pelleted, and resuspended in 100% ethanol. To monitor genome-wide damage-induced cohesion, we used the Tet-operators/Tet-repressor-GFP ("Tet-O/TetR-GFP") system that utilizes a Tet-operator array inserted at the *URA3* locus, 35 kb from the chromosome V centromere, which endogenously expressed GFP tagged Tet-repressors bind to. Separation of two fluorescent foci in a G_2/M-arrested cell indicates separated sisters, *i.e.*, deficient damage-induced cohesion. The experimental set up is illustrated in Figure 6A. Each mutant was tested at least twice and at least 200 cells were counted for each time point.

Purification of GST-tagged recombinant proteins

The *RAD30* and *ECO1* ORFs were amplified with PCR and integrated into the pGEX-4T-3 vector to generate glutathione S-transferase (GST)-tagged proteins with a thrombin site. Two times YT medium (yeast extract, tryptone, NaCl, and 0.3 mM isopropyl β-D-1-thiogalactopyranoside; Thermo Fisher Scientific) was used for expression of recombinant Polη in BL21 at 25° for 6–8 hr, or Eco1 in C41 (DE3) at 30° for 3 hr. GST-tagged proteins were purified on glutathione sepharose 4B resin (GE Healthcare), followed by thrombin (Sigma, St. Louis, MO) cleavage for 3 hr at 21°. Eluates were then concentrated through Vivaspin columns (Sartorius Stedim), and buffer was changed to kinase buffer (20 mM Tris-Cl pH 7.5, 50 mM NaCl, 1 mM $MgCl_2$, 0.5 mM EDTA, 20% glycerol, 0.01% Triton X-100, and 2 mM DTT) for the *in vitro* kinase assay; or HAT buffer (50 mM Tris-Cl pH 8.0, 50 mM NaCl, 2.5 mM $MgCl_2$, 0.1 mM EDTA, 5% glycerol; supplemented with 1mM PMSF, 1 mM DTT, 10 mM sodium butyrate, and 5 μM TSA) for *in vitro* acetylation assay. Protein concentrations were measured with a Bradford assay.

In vitro kinase assay

Purified recombinant Polη-GST or *Polη-3A*-GST (0.8 μg) was co-incubated with the Clb2-HA/Cdc28 complex, immunoprecipitated from yeast whole-cell extracts (Lyons and Morgan 2011), in kinase buffer, with or without γ-^{32}P-ATP for 15 or 30 min. The reaction was stopped by adding 4× SDS sample buffer. Recombinant human histone H1 (4 μg per reaction) was used as positive control (New England Biolabs, Beverly, MA). The samples were separated by SDS-PAGE and analyzed with autoradiography.

In vitro acetylation assay

Purified recombinant GST-tagged Polη (6 μg) and Eco1 (12 μg), were mixed with 1 μl of ^{14}C-acetyl-coenzyme A (^{14}C-CoA; 60 mCi/mmol; PerkinElmer, Norwalk, CT) in HAT buffer (final 25 μl), and incubated for 4 hr at 35°. Samples were then boiled in SDS sample buffer (2×) and analyzed by Coomassie staining or autoradiography after separation on SDS-PAGE. Samples for mass spectrometry analysis were prepared as above, except using unlabeled acetyl-CoA (Roche). After gel purification, protein samples were analyzed by nanoliquid chromatography-tandem mass spectrometry (nLC-MS/MS).

Purification of FLAG-tagged Polη to identify acetylation sites in vivo

To purify FLAG-tagged Polη (Polη-FLAG), 4 liters of yeast cells cultured in YEPR were grown to OD_{600} 1.8. Benomyl (final 80 μg/ml) was added and when cells reached G_2/M,

two liters of cells were harvested as the "minus break" sample. Galactose (final 2%) was added to the remainder to induce DSBs by P_{GAL}-*HO* on chromosome III, and chromosome VI with an ectopic integrated HO site. The remaining cells were collected as the "plus break" sample after 90 min. Cell pellets were then frozen with liquid nitrogen and stored at −80° until preparation of whole-cell extracts. Thawed pellets were resuspended in lysis buffer (25 mM HEPES-NaOH pH 7.9, 400 mM NaCl, 10% glycerol, 0.1% Triton X-100, 1 mM DTT, 1 mM PMSF, 10 mM sodium butyrate, protease inhibitor cocktail, and phosphatase inhibitor cocktail) and lysed in a 6870 freezer mill (SPEX, CertiPrep). Whole-cell extracts were cleared by centrifugation at 17,000 *g* for 30 min. The soluble fraction was incubated with equilibrated M2-FLAG affinity resin (Sigma) at 4°, and rotated overnight to immunoprecipitate Polη-FLAG. The M2-FLAG affinity resin was then washed once with lysis buffer and Polη-FLAG was eluted through 3XFLAG peptide (Sigma) competition. Eluates were precipitated with TCA, resuspended in 8 M urea, and run on SDS-PAGE, followed by Coomassie staining before gel purification and nLC-MS/MS analysis.

In-gel digestion of Coomassie-stained gel bands

Tryptic digestion was performed by a liquid-handling robot (MultiProbe II; PerkinElmer), including protein reduction in 10 mM DTT and alkylation in 55 mM iodacetamide. Gel pieces were dehydrated in 100% acetonitrile, and digested for 5 hr at 37° with trypsin (13 ng/μl).

Mass spectrometry analysis

nLC-MS/MS analysis was performed using an Easy-nLC system (Thermo Fisher Scientific) directly coupled to a hybrid LTQ Orbitrap Velos ETD mass spectrometer (Thermo Fisher Scientific). Peptides were separated in a 10-cm fused Silica Tip column (New Objective, Inc.) that was in-house packed with 3 μm C18-AQ ReproSil-Pur (Dr. Maisch GmbH), using a linear gradient from 3% to 48% acetonitrile in 42 min with flow rate 300 nl/min. The two mass-spectrometry acquisition methods were both comprised of one survey full scan, ranging from m/z 300 to m/z 2000, acquired in the FT-orbitrap with a resolution of R equal to 60,000 at m/z 400, followed by either up to 10 data-dependent collision-induced dissociation MS2 scans in profile mode, or pairs of electron-transfer dissociation/higher-energy collisional dissociation scans of up to five precursor ions with charge state ≥2.

Mass spectra database search

Tandem mass spectra from the LTQ Orbitrap Velos were extracted using Raw2MGF (in-house software), and the resulting mascot generic files from each gel lane were searched by Mascot Daemon 2.3.0 search engine (Matrix Science Ltd.). The search engine was set to search the SwissProt protein database (selected for *S. cerevisiae*, version 2013.04), using trypsin and two missed cleavage sites. Peptide mass tolerance was set to 10 ppm, 0.25 Da for the collision-induced dissociation and electron-transfer dissociation fragment ions, and 0.05 Da for higher-energy collisional dissociation fragment ions. Cysteine carbamidomethylation was specified as a fixed modification, whereas methionine oxidation; asparagine and glutamine deamidation; lysine, serine, histidine, tyrosine, and threonine acetylations; as well as serine, threonine, and tyrosine phosphorylation were defined as variable modifications. Post-translational modifications were verified by calculating A-Score and localization probability using Scaffold PTM 1.1.3 (Proteome Software). Peptides with localization score ≥90%, or with Mascot scores >30 were further considered. For identification of Polη acetylation sites *in vivo*, only DSB-specific acetylations were selected.

In situ immunofluorescence staining

Wild-type (WT) and Polη mutants were overexpressed by integration of the *GAL* promoter upstream of respective ORF, except the *Polη-S14A* mutant, for which the constitutive strong *GPD* or *ADH* promoter was utilized. To compare nuclear accumulation with and without break induction, isogenic strains with or without the P_{GAL}-*HO* allele were prepared. Cells were fixed with formaldehyde (final 3.7%) and spheroplasts were prepared through zymolyase treatment. The spheroplasts were subsequently applied on poly-L-lysine precoated slides, and fixed with ice-cold methanol followed by acetone, before blocking (3% BSA in 1× PBS). Cells were then stained with either anti-FLAG or anti-Myc primary antibody at 4° overnight. After 10 washes with blocking solution, the slides were incubated in the dark for 1 hr with Alexa Fluor 555-conjugated anti-mouse secondary antibody (Invitrogen, Carlsbad, CA). Finally, the slides were washed 10 times with blocking solution, once with 1× PBS, and then mounted with ProLong Gold or ProLong Diamond including DAPI. An untagged strain and secondary antibody alone were included as controls. Image overlays were generated with the Openlab software (Improvision) or with ImageJ. The experiment was repeated at least twice and at least 200 cells of each sample from individual experiments were assessed.

Flow cytometry

To confirm G_1 or G_2/M arrest, cells were pelleted and fixed with 70% ethanol (kept at 4° overnight) before RNase treatment (final 240 μg/ml; in 50 mM Tris-HCl, pH 7.8 at 37° overnight). Cells were then pelleted and resuspended in buffer containing 200 mM Tris-HCl, pH 7.5, 211 mM NaCl, and 78 mM $MgCl_2$ with propidium iodide (final 100 μg/ml). Cells were then sonicated before analysis with Becton Dickinson FACS Calibur, with 10,000 cell counts per sample.

Pulsed-field gel electrophoresis

To monitor break induction, samples were collected from damage-induced cohesion experiments before, and 1 hr after galactose addition. DNA plugs were prepared and run on 1% pulsed-field grade agarose gel with Bio-Rad CHEF-DR III as described (Desany *et al.* 1998). Initial switch time was set to

35.4 sec and the final to 83.6 sec, with 120° switching angle for optimal separation of chromosomes in the size range of chromosomes III and VI. The gel was run at 6 V/cm, at 14° for 24 hr.

Protein extractions and Western blotting

Protein extracts were prepared through glass bead disruption, with buffer containing 20 mM Tris-Cl, pH 8, 10 mM $MgCl_2$, 5% glycerol, 0.3 M ammonium sulfate, 1 mM EDTA, 1 mM DTT, 1 mM PMSF, and protease inhibitor cocktail tablet. Bolt 4%–12% Bis-Tris gels (Invitrogen) were used for electrophoresis and the Trans-blot Turbo system (Bio-Rad, Hercules, CA) for protein transfer. Membrane blocking and incubation with antibodies were performed with general procedures.

In silico modeling of Polη in complex with Cdc28

A homology model of *S. cerevisiae* Cdc28 was generated using SWISSMODEL (Waterhouse *et al.* 2018) from a cocrystal complex of human CDK2/Cyclin A and a target peptide (1QMZ; Brown *et al.* 1999). The target peptide in 1QMZ was then used as a reference to approximately orient the CDK consensus motif in a structure of DNA-bound Polη (2R8J; Alt *et al.* 2007) to have a canonical CDK-substrate interaction mode. The manual modeling was performed in COOT (Emsley and Cowtan 2004). The resulting draft model was thereafter energy minimized using PHENIX (Liebschner *et al.* 2019). The interface area was calculated as the difference in total accessible surface areas of isolated and interfacing structures divided by two as implemented in the PISA server (Krissinel and Henrick 2007).

Statistical analysis

One-way ANOVA, Scheffe *post hoc* test was used to assess statistical significance ($\alpha = 0.05$ or 0.1); analyzed with SPSS statistics software (IBM). Error bars represent SD.

Data availability

All data and methods required to confirm the conclusions of this work are within the article, figures, and supplemental materials. Strains and plasmids used in this study are listed in Tables S1 and S2, respectively. Primer sequences are available upon request. Supplemental material available at figshare: https://doi.org/10.25386/genetics.13055816.

Results

Polη is a substrate of the Cdc28 kinase in vitro

To better understand the regulation of Polη during its noncanonical, polymerase-independent role in formation of genome-wide damage-induced cohesion (Enervald *et al.* 2013), we sought to identify potential Polη regulators. By protein sequence, Polη appears to be a Cdc28 (Cdk1) substrate, containing two full and one partial CDK consensus motifs (Nigg 1993); where the S14, T612, and T547 residues would be the phosphorylation sites (Figure 1A). To test if Polη can be phosphorylated by Cdc28, we performed an *in vitro* kinase assay where a *Polη-3A* mutant, with all the three potential Cdc28 phosphorylation sites mutated to alanine, was compared with WT Polη. Cdc28 was purified through co-immunoprecipitation of the HA-tagged Clb2, the cyclin expressed during G_2/M phase. In addition, recombinant human H1 was included as positive control (Lyons and Morgan 2011). The *in vitro* assay showed that the purified WT Polη was phosphorylated only in the presence of both the Cdc28/Clb2 complex and radiolabeled γ-^{32}p-ATP. Importantly, phosphorylation of Polη was completely abolished when the three putative phosphorylation sites were mutated to alanine, implicating that one or more of these residues are the Cdc28 targets (Figure 1B).

Supporting the kinase assay result, we found when modeling a heterodimer constituted of *S. cerevisiae* Polη and a homology model of Cdc28, that Cdc28 and Polη could potentially form a complex with an interface area of ~1900 Å^2 (Figure 1C). The interface is located distant to substrate DNA and the polymerase active site. Furthermore, S14 on Polη could be modeled in position for phosphorylation, situated right by the γ-phosphate in the modeled Cdc28 kinase active site. In addition, the loop containing the basic P+3 residue in the phosphorylation motif, here K17, is relaxed in our minimized protein complex model, compared to the template structure of DNA-bound Polη (PDB: 2R8J; Alt *et al.* 2007). In this relaxed position, K17 is able to interact with the phospho-T169 in Cdc28 required for kinase activity (Cross and Levine 1998). Potential interactions between Cdc28 and Polη-T547 or Polη-T612 could not be modeled since a complete structure for the Polη C terminus is not available (Powers *et al.* 2018). Taken together, our *in vitro* and modeling results indicate that Polη is a target for Cdc28 phosphorylation.

Preventing Polη-S14 phosphorylation affects protein level, but has no effect on Polη TLS activity

In both yeast and human cells, Polη protein level is cell cycle regulated, peaking in G_2/M phase (Plachta *et al.* 2015; Bertoletti *et al.* 2017). Since phosphorylation by Cdc28 regulates protein stability (Hall *et al.* 2008), we asked whether Cdc28-mediated phosphorylation affects abundance of Polη in G_2/M. We found that among the three individually mutated sites, only the *Polη-S14A* mutation caused reduced protein level in G_2/M phase. Interestingly, such reduction was not observed when the other two putative phosphorylation sites were mutated simultaneously with S14 (*Polη-3A*) (Figure 2A). Furthermore, accompanied with reduced protein levels in the *Polη-S14A* single and *Polη-S14A T612A* double mutants, an additional band ~40 kDa was observed, possibly representing a Polη degradation or cleavage product (Figure S1, A and B; see also *Discussion*).

By affecting abundance of the full-length protein, *S14A* could potentially act as a null allele if the absolute Polη level is important. Furthermore, preventing phosphorylation of any of the potential phosphorylation residues could independently influence protein functionality. To test this, we first

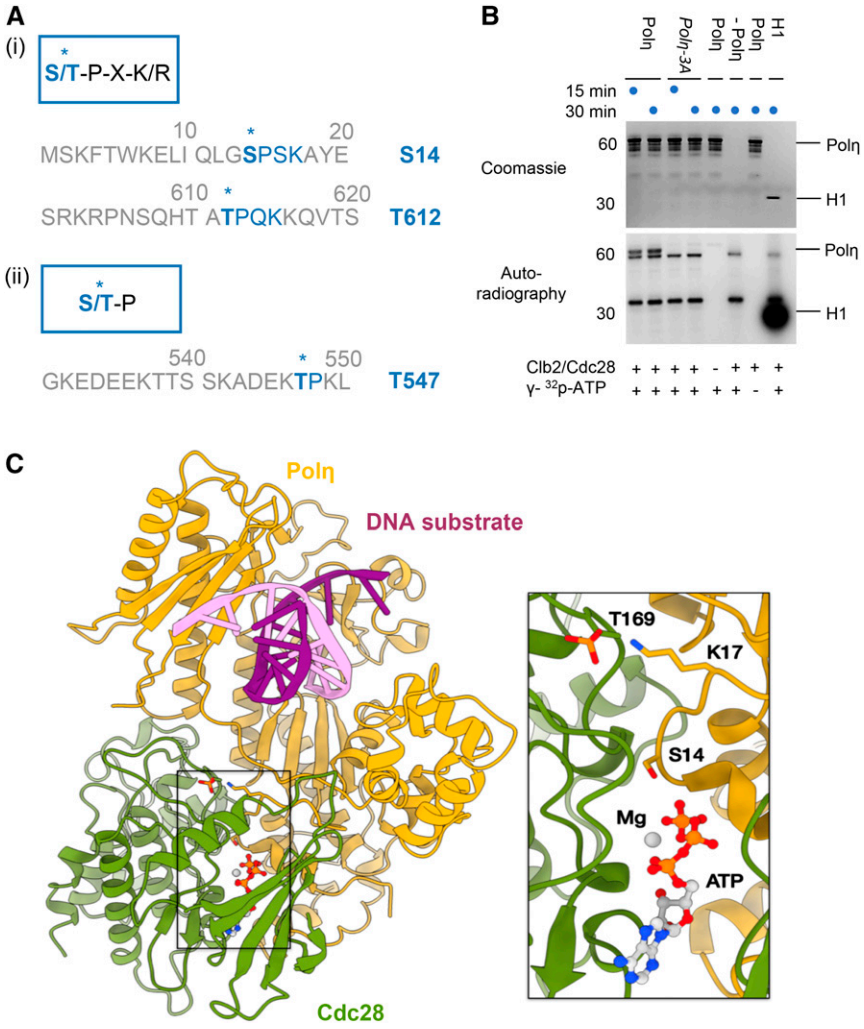

Figure 1 Polη is a substrate of the Cdc28 kinase *in vitro*, supported by *in silico* modeling. (A) Polη contains three CDK consensus motifs (in blue). The putative phosphorylation sites are bold, marked with asterisks and shown with numbers; (i) complete CDK consensus motif, (ii) partial CDK consensus motif. (B) Cdc28-Polη *in vitro* kinase assay. Purified recombinant Polη-GST or *Polη-3A*-GST (Polη with the three putative phosphorylation sites mutated to alanine) were incubated with purified Cdc28/Clb2, in the presence or absence of ^{32}P-γATP, for 15 or 30 min (indicated with filled blue circles). Recombinant human H1 was used as positive control. The kinase assay was repeated three times. (C) *In silico* modeling of Polη in complex with Cdc28. Protein docking of a Cdc28 homology model (green) and Polη (yellow), with bound DNA (pink/violet). Inset: Close-up of the Cdc28 active site showing Polη-S14 positioned close to the modeled ATP's γ-phosphate (modeled ATP in gray with standard atom coloring). This minimized theoretical heterodimer model indicates that the Polη-K17 can interact with the Cdc28 phosphor-T169, crucial for kinase activity. CDK, cyclin-dependent kinase.

examined if the single *Polη-S14A*, *T547A* or *T612A* mutations would render cells sensitive to UV irradiation. In contrast to the UV-sensitive Polη null mutant (*rad30*Δ), the Polη-phosphorylation mutants were as viable as WT cells (Figure 2B), indicating that the cells ability to efficiently bypass UV damages does not depend on phosphorylation of these residues. From this we conclude that Cdc28-mediated S14 phosphorylation is a potential mechanism for Polη stabilization in G_2/M phase, but has no effect on Polη TLS function.

Eco1, cohesin, and Polη are all required for cell survival after UV irradiation

In addition to Cdc28, we speculated that Eco1, the acetyltransferase required for establishment of cohesion, could interact with or regulate Polη. This was based on several indications. First, Eco1 overexpression rescues cells void of Polη in formation of damage-induced cohesion (Enervald *et al.* 2013), suggesting a functional or genetic interaction. Second, it is noteworthy that the Eco1 ortholog in *Schizosaccharomyces pombe* (Eso1) is expressed as a fusion protein with Polη (Madril *et al.* 2001). As a start, we investigated whether Polη and Eco1 would interact genetically for Polη's canonical role in bypassing UV-induced DNA lesions. Since the *eco1*Δ null mutant is lethal, and several identified *eco1 ts* alleles easily gain revertants, we chose to use an *eco1*Δ*rad61*Δ strain for the epistasis analysis. Deleting Wpl1 (encoded by the *RAD61* gene), allows simultaneous Eco1 deletion (Rolef Ben-Shahar *et al.* 2008; Unal *et al.* 2008; Rowland *et al.* 2009). As expected, the *rad30*Δ cells showed dose-dependent UV sensitivity (Figure 3, A–C). In contrast, deleting the *RAD61* gene did not result in any obvious effect on cell survival after UV exposure, although the *rad30*Δ*rad61*Δ double mutant showed a subtle decrease in viability at 30 J/m^2 (Figure 3A). The *eco1*Δ*rad61*Δ mutant displayed UV sensitivity already at low-irradiation dose (12 J/m^2, Figure 3A). Notably, simultaneous *RAD30* deletion greatly enhanced UV sensitivity of the *eco1*Δ*rad61*Δ mutant at high doses (24 and 30 J/m^2), the doses where the effect of UV irradiation on the *rad30*Δ single mutant can be seen.

Furthermore, we analyzed the possible genetic interactions between Polη and the cohesin loader Scc2, as well as the cohesin subunits Scc1 and Smc1. Since these are all essential,

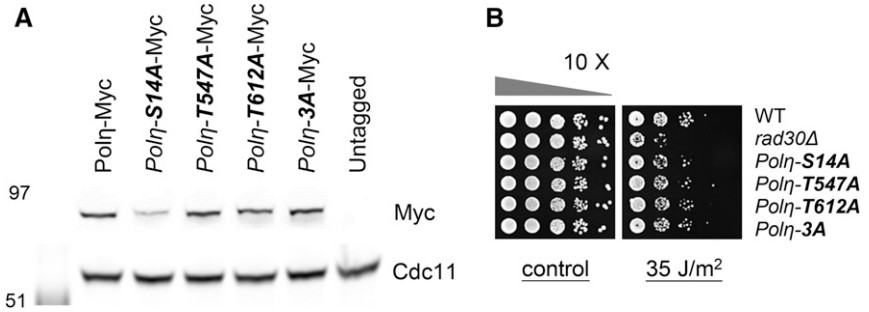

Figure 2 The *Polη-S14A* mutation affects protein level, but not TLS activity. (A) Protein levels of Myc-tagged Polη-phosphorylation mutants in G_2/M phase. Cdc11 was used as loading control. (B) UV spot assay of Polη single and triple phosphorylation mutants. Tenfold serial dilutions of midlog phase cells were spotted on YEPD plates and exposed to 35 J/m^2 UVC. Plates were documented after 3 days. YEPD, YEP media with glucose.

we used the respective *ts* alleles (Michaelis *et al.* 1997) for epistasis analyses. Restrictive temperatures, however, resulted in almost complete loss of viability following UV irradiation (Figure S2). Since genetic interactions were not possible to determine under such conditions, semipermissive temperatures were applied. As can be seen in Figure 3, B and C, *scc2-4*, *scc1-73*, and *smc1-259* were all sensitive to UV irradiation even at a low dose (12 J/m^2). Similar to the *eco1*Δ*rad61*Δ*rad30*Δ mutant, *RAD30* deletion in these cohesin *ts* mutants resulted in additive effects on their UV sensitivities at higher doses (Figure 3, B and C). Loss of functional Eco1, or any of the cohesin subunits, together with loss of Polη activity, were in all cases additive. These results clearly show that the cohesin network is, like Polη, important for the response to UV damage, albeit acting in a different pathway from that of Polη.

Polη is a substrate of Eco1 in vitro

Although Polη and Eco1 appeared to act separately in response to UV irradiation, the possibility that Eco1 acetylates Polη for formation of damage-induced cohesion cannot be ruled out, since the latter does not depend on Polη as a TLS polymerase (Enervald *et al.* 2013). Thus, we continued with investigating whether Polη can be targeted for acetylation by Eco1 *in vitro*. To this end, we incubated purified Polη-GST alone or together with purified recombinant Eco1-GST, in the absence or presence of ^{14}C-CoA. This indeed showed efficient acetylation of Polη by Eco1 in the presence of ^{14}C-CoA (Figure 4A), and that Eco1 was autoacetylated as previously reported (Ivanov *et al.* 2002). To identify the Eco1-mediated Polη acetylation sites, we coupled the *in vitro* acetylation assay with mass spectrometry analysis. Again, Polη-GST was purified and incubated *in vitro* with and without recombinant Eco1-GST, as described but with unlabeled acetyl-CoA. Gel-purified Polη samples were then analyzed by mass spectrometry. The identified residues are depicted in Figure 4B in green, and further described below.

Since DNA damage has been suggested to trigger Eco1-mediated acetylation of PCNA (Billon *et al.* 2017), and the cohesin subunit Scc1 (Heidinger-Pauli *et al.* 2009), we were inspired to investigate if Polη was acetylated *in vivo* in response to DNA damage. WT Polη-FLAG was immunoprecipitated from whole-cell extracts, before and after DSB induction (P_{GAL}-*HO*) in G_2/M-arrested cells, and subsequently analyzed by mass spectrometry to identify modified residues. The DSB-specific acetylations that appeared *in vivo* are depicted in Figure 4B, in blue. The complete mass spectrometry analysis results are shown in the Supplemental Material (Table S3, Files S1 and S2), and the selection criteria are described in the *Materials and Methods*.

The acetylation sites were widely distributed across the Polη coding sequence, in different functional domains such as the catalytic domain, the ubiquitin-binding/zinc-finger motif, and the putative bipartite nuclear localization sequence (NLS; 602–617 amino acids) at its C-terminal (Kannouche *et al.* 2001). The Eco1-mediated (*in vitro*) and the DSB-specific (*in vivo*) residues showed very limited overlap. This could suggest that the Eco1-mediated acetylations identified *in vitro* are not triggered by DNA DSBs. That the DSB-induced Polη acetylations, detected *in vivo*, were not identified as Eco1 targets in the *in vitro* acetylation assay could either mean that they are catalyzed by another acetyltransferase, or are Eco1 targets but require other factors and/or modifications present *in vivo* but not *in vitro* for acetylation.

Polη-KR mutations affect Polη nuclear accumulation, protein level, and TLS activity

To investigate if the Eco1-mediated (*in vitro*) and DSB-specific (*in vivo*) acetylation sites are biologically important, single lysine to arginine (KR) point mutants were generated according to the mass spectrometry results (depicted in Figure 4B). We then examined if these acetylation sites contributed to generation of damage-induced cohesion, but found that none of the tested single *Polη-KR* mutants were deficient (data not shown). We speculated that the effect of single *Polη-KR* mutations could be masked by compensatory acetylations, and therefore focused on *Polη-multiple KR* mutants. From the *in vitro* identified Eco1-mediated acetylation residues, the K17, K546, K603, and K615 residues were selected for further analyses, as they were close to the potential Cdc28-phosphorylation sites (S14, T547, and T612). This resembled Scc1-K84, next to the potential phosphorylation site Scc1-S83, which are both important for damage-induced cohesion (Heidinger-Pauli *et al.* 2009). Thus, we generated the *Polη-K17R K546R K603R* and *Polη-K17R K546R K615R* triple mutants, referred to as "*Polη-triple KR*" mutants. In addition, in an unbiased approach, we generated a "*Polη-in vitro KR*" allele based on the identified Eco1-mediated

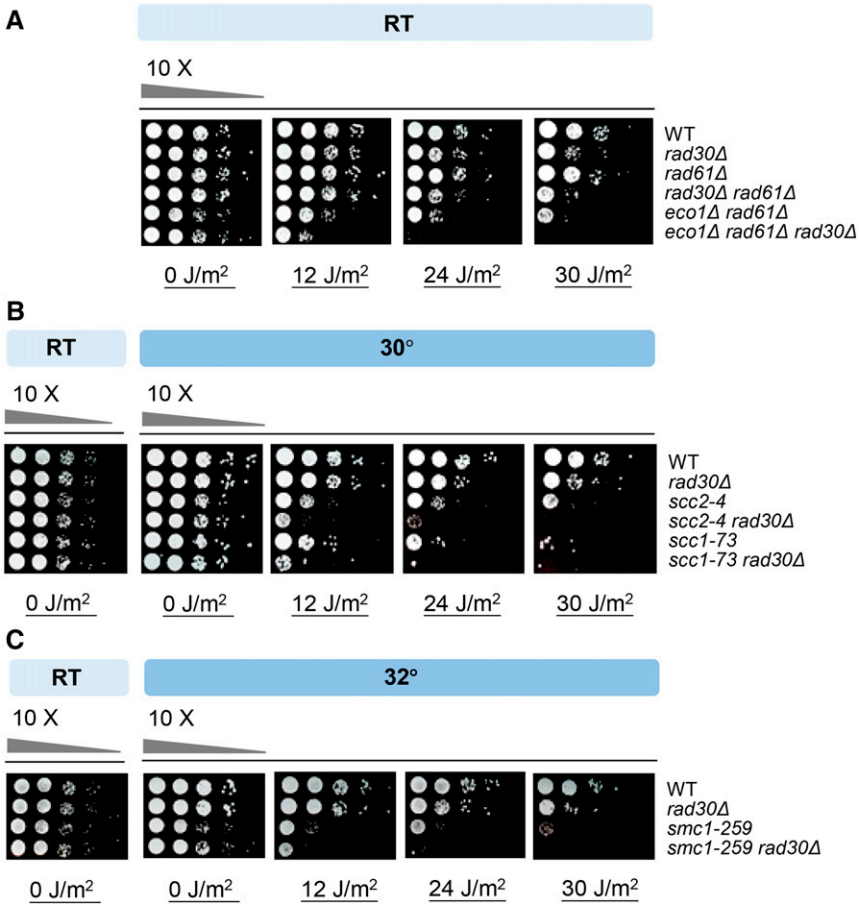

Figure 3 Eco1, cohesin, and Polη are required for cell survival after UV irradiation. (A–C) Tenfold serial dilutions of midlog phase cells were spotted on YEPD, with or without follow-on UVC exposures. Semipermissive temperatures for the temperature-sensitive cohesin loader and cohesin subunits mutants were used: 30° for *scc2-4* and *scc1-73*, and 32° for *smc1-259*. Plates were documented on the second or third day. One representative experiment from two independent assays performed is shown. RT, room temperature.

acetylations from the *in vitro* assay, and a "*Polη-in vivo KR*" allele containing mutations of the identified DSB-specific acetylations (see Figure 4B, in green and blue, respectively).

Because the K603 and K615 residues are located within the putative NLS motif, and acetylated lysines within an NLS regulate nuclear localization (Cao *et al.* 2017), we decided to first examine nuclear accumulation of the *Polη-triple KR* mutants by *in situ* immunofluorescence staining. Since the normal Polη protein level was too low to generate a robust immunofluorescence signal (data not shown), we utilized the inducible GAL promoter for overexpression of endogenous FLAG-tagged WT and various *Polη KR* mutants. This improved Polη visualization and resulted in 70%–90% of cells scoring positive for α-FLAG staining (data not shown). As the *Polη-in vivo KR* allele was generated based on modifications found after DSB induction, we were also interested in investigating possible DSB dependent nuclear accumulation. The cells were arrested in G_2/M, in the presence of galactose for Polη overexpression and DSB induction (in the strains harboring the P_{GAL}-*HO* allele). Cells with distinct Polη staining (anti-FLAG), clearly colocalizing with the DAPI signal (the nucleus) were defined as positive for nuclear accumulation. On the contrary, cells with a fuzzy, evenly distributed Polη staining throughout the cells were scored negative (Figure 5A). Approximately 90% of the cells expressing WT Polη displayed nuclear accumulation, with and without break induction. As suspected, the two *Polη-triple KR* mutants and the *Polη-in vitro KR* mutant showed either largely reduced or abolished nuclear accumulation, while that of the *Polη-in vivo KR* mutant was not significantly affected (Figure 5B).

In parallel, we noticed that the Polη steady-state level was affected by the two *Polη-triple KR* and the *Polη-in vivo KR* mutations (Figure 5C). In contrast, the *Polη-in vitro* KR mutant appeared to be more stable than the two *Polη-triple KR* mutants, despite containing the same mutations (*K17R*, *K546R*, *K603R*, and *K615R*), suggesting that some potential acetylation residues identified from the *in vitro* assay counteract others for Polη stabilization.

Reduced protein levels of the two *Polη-triple KR* mutants, and compromised nuclear accumulation of the *Polη-triple KR* as well as the *Polη-in vitro KR* mutants, could indicate that Eco1 is required for Polη stability and nuclear localization. To test this, we monitored nuclear accumulation and protein level of WT Polη in the absence of Eco1, in G_2/M phase. However, Polη nuclear accumulation and protein level were not significantly affected in neither the *rad61*Δ nor the *eco1*Δ*rad61*Δ mutant (Figure 5, D and E). Instead, these results suggest that the disrupted NLS indeed compromise nuclear accumulation of the *Polη-triple KR* and *Polη-in vitro KR* mutants, independently of Eco1.

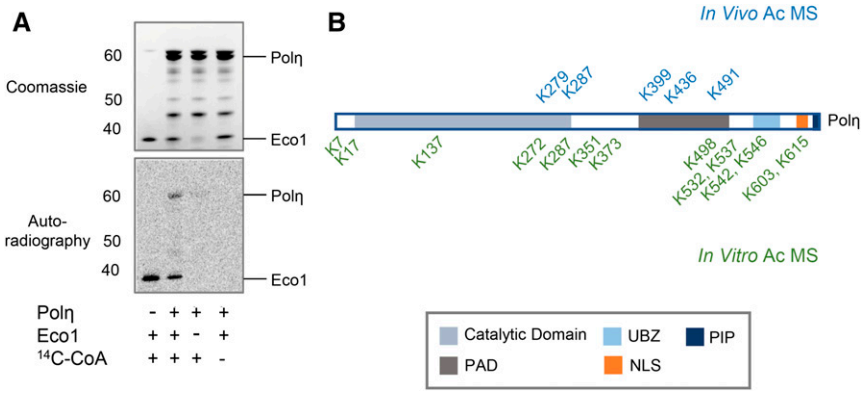

Figure 4 Polη is an Eco1 substrate *in vitro*. (A) *In vitro* acetylation assay. Purified recombinant Polη was incubated with or without purified recombinant Eco1, in the presence or absence of ^{14}C-acetyl-coenzyme A (^{14}C-CoA), and acetylation was visualized by autoradiography. (B) Mass spectrometry detected *in vitro* (Eco1-mediated) and *in vivo* (DSB-specific) acetylation sites are shown in green and blue, respectively. DSB, double-strand break; NLS, nuclear localization sequence; PAD, polymerase-associated domain; PIP, PCNA-interacting protein motif; UBZ, ubiquitin-binding/zinc-finger motif.

Besides, similar to the Polη-phosphorylation mutants, we were interested in knowing if any of the lysines identified as acetylation targets were important for the canonical TLS activity of Polη. As expected, the *Polη-multiple KR* mutants with affected nuclear accumulation showed increased UV sensitivity (Figure 5F). However, despite being proficient in nuclear accumulation, expression of *Polη-in vivo KR* sensitized cells to UV irradiation (Figure 5, A, B, and F). To rule out the possibility that UV sensitivity of *Polη-in vivo KR* was due to reduced protein level (Figure 5C), the constitutive strong *ADH* promoter was integrated upstream of the *Polη-in vivo KR* coding sequence. Although the P_{ADH}-*Polη-in vivo KR* expression did not reach the level of WT Polη controlled by the *ADH* promoter (P_{ADH}-Polη), it was markedly enhanced compared to its endogenous level (Figure 5G). We then noted that constitutively increased expression of WT or mutated *Polη* did not perturb normal cell growth (Figure S3A; control). Elevated expression of the *Polη-in vivo KR* allele under the *ADH* promoter clearly reduced, but did not fully rescue the UV sensitivity of this mutant (Figure S3A). This indicated that the UV sensitivity of the *Polη-in vivo KR* mutant predominantly was due to reduced protein level, but partly also a consequence of one or several of the mutated residues (K279, K287, K399, K436, K491). These results together indicate that post-translational modification of selected lysine residues contribute to proper nuclear accumulation of Polη, regulates its protein steady-state level, and is important for Polη TLS activity.

Poln-S14 is important for establishment of damage-induced cohesion

Having characterized the *Polη-SA/TA* and *Polη-multiple KR* mutants described above, we were ultimately interested in knowing if these post-translational modifications were important for formation of damage-induced cohesion. We monitored generation of damage-induced cohesion as previously described (Ström *et al.* 2004, 2007; see also *Materials and Methods* and Figure 6A). Briefly, strains of interest, with *smc1-259* background, were arrested in G_2/M. DSBs (P_{GAL}-*HO*) were subsequently induced by addition of galactose, which simultaneously activated expression of ectopic P_{GAL}-*SMC1-MYC*. The TetO/TetR-GFP system was used for determination of sister separation. Proper G_2/M arrest, efficiency of break induction, and protein expression of P_{GAL}-Smc1-Myc were also confirmed. Examples of such controls can be found in Figure S4.

Since monitoring damage-induced cohesion includes a prolonged G_2/M arrest, it was possible that the deficient damage-induced cohesion observed in *rad30*Δ cells reflected a cohesion maintenance defect. To exclude this possibility, before proceeding, we monitored sister chromatid cohesion maintenance in *rad30*Δ cells, and concluded that no defect in cohesion maintenance could be noticed in *rad30*Δ cells (Figure S5B). Thus, the deficient damage-induced cohesion in *rad30*Δ cells is not due to lack of cohesion maintenance.

We then choose to investigate if the *Polη-in vivo KR* mutant could establish damage-induced cohesion, since these acetylations were identified as DSB specific, and that this mutated Polη in principle was proficient in nuclear accumulation (Figure 4B and Figure 5, A and B). Because of reduced protein level of the *Polη-in vivo KR* under control of its endogenous promoter, we again expressed it from the *ADH* promoter. Compared to WT Polη (P_{ADH}-*Polη*), the P_{ADH}-*Polη-in vivo KR* mutant did not show deficiency in damage-induced cohesion, indicating that none of the K279, K287, K399, K436, or K491 residues are important for the same (Figure 6B).

Regarding the putative Cdc28-mediated phosphorylation of Polη, we first tested the abilities of *Polη-SA/TA* single mutants for generation of damage-induced cohesion. We found that while the *Polη-T547A* and *Polη-T612A* mutants were not deficient, the *Polη-S14A* mutant showed similar degree of sister separation as the *rad30*Δ null mutant (Figure 6C). Despite our finding that reduced protein level of the *Polη-S14A* mutant (Figure 2A) did not impede Polη TLS activity (Figure 2B), the ability to establish damage-induced cohesion could potentially be more sensitive to reduced Polη protein level. Thus, to directly test if the *Polη-S14 is* required for damage-induced cohesion, regardless of the reduced protein level, we integrated the *ADH* promoter also in front of the *Polη-S14A* coding sequence. The resulting protein level was similar to the WT Polη under the *ADH* promoter (P_{ADH}-*Polη*) (Figure 6D); however, this was not sufficient for *Polη-S14A* to

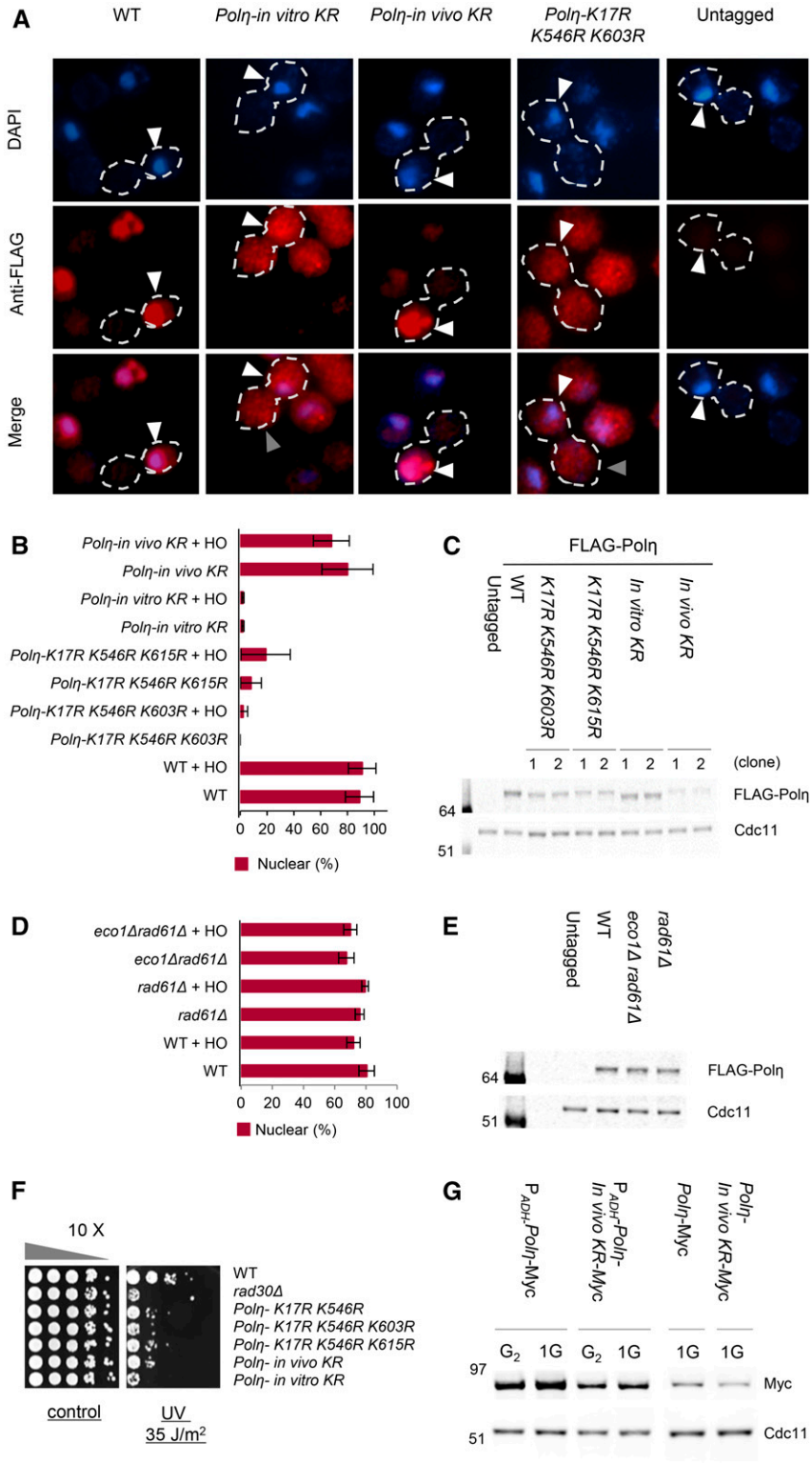

Figure 5 *Polη-KR* mutations affect nuclear accumulation and total protein level. (A) Representative *in situ* immunofluorescence images of indicated WT or mutated FLAG–Polη, stained with anti-FLAG and counterstained with DAPI. Nuclear accumulation of Polη after break induction in G_2/M phase was determined by colocalization of anti-FLAG and DAPI signals, indicated by white arrows. Nonnuclear staining with anti-FLAG (Polη) is indicated by gray arrows. (B) Percent of cells that expressed FLAG-Polη at detectable level and showed nuclear accumulation, with and without break induction in G_2/M phase. Quantified from *in situ* stained cells. Means ± SD from at least two independent experiments are shown. (C) Protein levels of FLAG-Polη with indicated KR mutations (asynchronized cells). Numbers one and two indicate two different transformation clones. Cdc11 was used as loading control. (D) Polη nuclear accumulation in the absence of Eco1 and/or Wpl1. Quantified as in B. Means ± SD from at least two independent experiments are shown. (E) Protein levels of FLAG-Polη in G_2/M phase, in the presence or absence of Eco1 and/or Wpl1. Cdc11 was used as loading control. (F) Spot assay to monitor UV sensitivities of the *Polη-KR* mutants. Tenfold serial dilutions of midlog phase cells were spotted on YEPD plates, subsequently exposed to 35 J/m^2 UVC, and documented after 3 days. (G) Protein levels of Polη-Myc and *Polη-in vivo KR*-Myc, expressed from the endogenous or the constitutive strong *ADH* promoter. The samples were from the same gel, but the image was cropped to show selected samples. Cdc11 was used as loading control. 1G, 1 hr break induction by addition of galactose (P_{GAL}-*HO*); G_2, G_2/M arrested cells; HO, homothallic switching endonuclease; YEPD, YEP media supplemented with glucose.

generate damage-induced cohesion (Figure 6E), indicating that the actual phosphorylation of Polη-S14 residue is indeed required for formation of damage-induced cohesion.

In summary, post-translational modifications of the *Polη-in vivo* residues (K279, K287, K399, K436, and K491) do regulate protein level and TLS activity of Polη, but are not influencing generation of damage-induced cohesion. In contrast, among the three putative Cdc28 phosphorylation sites, Polη-S14 is clearly required for formation of damage-induced cohesion. These findings depict discrete functions of the

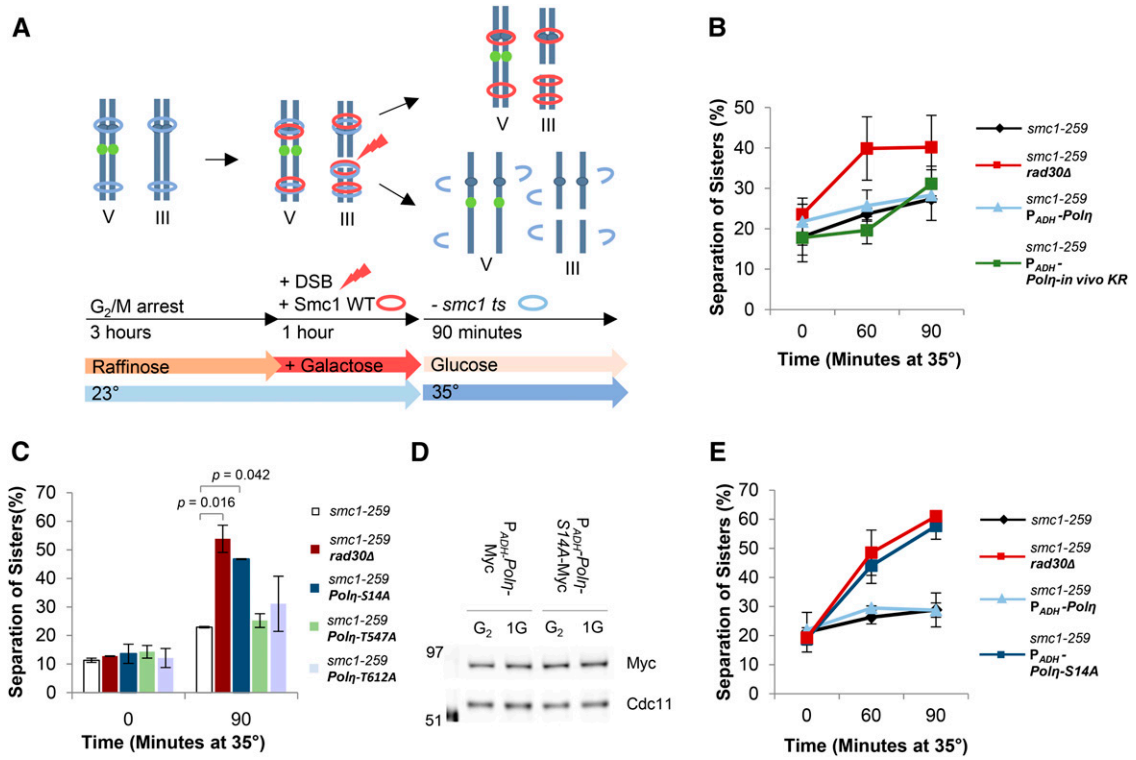

Figure 6 Polη-S14 is important for establishment of damage-induced cohesion. (A) A schematic experimental outline for a typical damage-induced cohesion experiment. Cells expressing the temperature-sensitive allele *smc1-259* (*smc1 ts*) are synchronized in G_2/M by addition of benomyl. Galactose is then added for expression of ectopic P_{GAL}-*SMC1* (Smc1 WT) and induction of DSBs on chromosome III (P_{GAL}-*HO*). After 1 hr, the temperature is raised to 35°, restrictive for *smc1-259*, whereby the cohesion established during S phase (blue rings) is destroyed. The Tet-O/TetR-GFP system (green dots) is used to monitor damage-induced cohesion (red rings) on chromosome V. (B) Damage-induced cohesion assay of P_{ADH}-*Polη-in vivo KR*. Means ± SD from at least two independent experiments are shown. (C) Damage-induced cohesion assay of indicated single Polη-phosphorylation mutants (S/T to A). Means ± SD from at least two independent experiments are shown. Statistically significant differences were analyzed with one-way ANOVA, Scheffe *post hoc* test ($P < 0.05$). (D) Protein levels of Polη-Myc and Polη-S14A-Myc, expressed from the *ADH* promoter. Cdc11 was used as loading control. (E) Damage-induced cohesion assay of P_{ADH}-*Polη-S14A*. Means ± SD from at least two independent experiments are shown. 1G, 1 hr break induction by addition of galactose (P_{GAL}-*HO*); DSBs, double-strand breaks; G_2, G_2/M arrested cells; HO, homothallic switching endonuclease.

identified Polη post-translational modifications, and provide new insights into regulation of Polη for generation of damage-induced cohesion.

Discussion

Similar to a previous study which identified Polη as a Cdc28 target through proteomic screening (Ubersax *et al.* 2003), we showed that Polη can be phosphorylated by Cdc28 *in vitro*. In addition, our structure modeling displayed a high degree of sterical complementarity, and indicated that the Polη-S14 residue is an attractive target for Cdc28. The putative binding mode features an interface area of ~1900 Å^2, which is well above the average for heterodimers of validated protein-protein complexes (Nooren and Thornton 2003). This interface area can also be compared to the 1200 Å^2 for a Polη homodimer, and the1600 Å^2 area for a human CDK2-Cyclin heterodimer (Brown *et al.* 1999; Alt *et al.* 2007).

Of the three mutated putative Cdc28 consensus residues, we found that S14 phosphorylation was required for formation of damage-induced cohesion, while Polη TLS activity was independent of this modification. We have so far not been able to directly detect Polη-S14 phosphorylation *in vivo*. We therefore wanted to investigate if Polη-S14 is a Cdc28 target *in vivo* through an alternative approach. Assuming that Cdc28 inactivation would cause deficient damage-induced cohesion, we planned to test if a Polη-S14 phosphomimic allele would be able to rescue such defect. However, this could not be done since Cdc28 inactivation caused premature loss of S phase established cohesion (data not shown), which was also in agreement with previous reports (Kitazono *et al.* 2003; Brands and Skibbens 2008).

Our results suggest that the Cdc28-mediated phosphorylation, which should be cell cycle regulated, could be important for the reported increased Polη abundance in G_2/M, due to stabilization (Plachta *et al.* 2015; Bertoletti *et al.* 2017). In addition, we observed a complex pattern of Polη cleavage or degradation, where the cleavage product was observed in *Polη-S14A* single and *Polη-S14A T612A* double mutants, but not in the *Polη-T547A* and *Polη-T612A* single mutants and the *Polη-3A* mutants. These results suggest that serial phosphorylation could act in concert to promote or prevent

Polη degradation. We suspect that phosphorylation of Polη-T547 could be a signal for Polη cleavage, which is antagonized by Polη-S14 phosphorylation (summarized in Figure S1C). Future investigations will be needed to test this, and to understand the temporal and spatial regulation of possible Polη cleavage.

In line with our finding that Cdc28-dependent phosphorylation was important for Polη function in response to damage, phosphorylation of human Polη after UV irradiation is required for localization to sites of lesions, and contributes to cell survival after UV exposure (Chen *et al.* 2008; Bertoletti *et al.* 2017; Peddu *et al.* 2018). As opposed to the human counterpart, however, nuclear accumulation of yeast Polη seems to be independent of the DNA damage response, since WT Polη and the *Polη-S14A* mutant both accumulated in the nucleus in the absence of break induction, and were insensitive to UV irradiation (Figures 2B and 5B and Figure S3).

When investigating a possible genetic interaction between Polη and proteins in the cohesin network, we found that cohesin mutants were highly sensitive to UV irradiation. In line with this, cohesin suppresses interhomolog recombination after UV exposure in budding yeast (Covo *et al.* 2010). In addition, fission yeast Rad21 (Scc1) is cleaved by separase after UV exposure, while noncleavable Rad21 results in slower repair of UV-induced thymine dimers (Nagao *et al.* 2004). These studies, together with our data, suggest that cohesin is indeed important for repair of UV-induced DNA damages. The additive sensitivity of *eco1*Δ*rad61*Δ cells and cohesin *ts* mutants in combination with *rad30*Δ, further suggests that not only cohesin, but also sister chromatid cohesion is required for repair of UV-induced lesions.

We showed that Polη is an Eco1 substrate *in vitro*, and identified putative Polη acetylation sites *in vitro* and *in vivo* for the first time. However, nuclear accumulation deficiency and reduced protein level observed in several *Polη-multiple KR* mutants turned out to be independent of Eco1-mediated acetylation. Although we cannot rule out the possibility that these lysine residues are substrates of alternative post-translational modifications, such as sumoylation or ubiquitination, identification of the authentic enzyme actually modifying these Polη residues for protein level and UV-repair competence could be an interesting future topic.

Genome-wide damage-induced cohesion on undamaged chromosomes might be argued to be a unique biological process in haploid budding yeast cells. However, studies in *Arabidopsis thaliana* and chicken DT40 cells propose that generation of damage-induced cohesion could be conserved [reviewed in Dorsett and Strom (2012)]. In addition, in HeLa cells, cohesin binding is reinforced in an ESCO1 (human Eco1)-dependent manner in response to ionizing radiation. This suggests that reactivation of cohesion establishment could also occur in mammalian cells (Kim *et al.* 2010). This concept is also supported by our observation that diploid yeast cells, which resemble higher eukaryotes with the presence of homologs, do generate damage-induced cohesion (data not shown).

In conclusion, our investigations of *Polη-KR* mutants provide better understanding of the Polη regulation for nuclear accumulation, protein level, and TLS activity. Most importantly, we have revealed that Polη can be a Cdc28 substrate. Polη-S14 phosphorylation not only regulates Polη protein level, but also contributes to formation of damage-induced cohesion. Further studies on Polη-S14 phosphorylation should in the future improve our understanding about how Polη contributes to establishment of damage-induced cohesion.

Acknowledgments

We thank C. Björkegren for sharing strains and plasmids, and T. Frisan for plasmids and BL21 bacteria. We also thank C. Björkegren, T. Kanno, and M. Scherzer for critical reading of the manuscript; as well as S. Åström and A. Kegel for advice. This work was supported by the Swedish Research Council (grant 2013-3566), the Swedish Cancer Society (grant 2014/573), the Bergvall Foundation (grants 2016-01868 and 2017-02287), and the Karolinska Institutet PhD student financing program (3-1818/2013) to L.S.

Author contributions: P.-S.W., E.E., and L.S. conceptualized the study. P.-S.W., E.E., A.J., C.P., D.R., and L.S. were responsible for study investigation. P.-S.W., E.E., D.R., B.M.H., and L.S. were responsible for study analysis. B.M.H. conducted the modelling. L.S. was responsible for study resources. P.-S.W. and L.S. wrote the manuscript. All authors read and commented on the manuscript.

Literature Cited

Acharya, N., K. Manohar, D. Peroumal, P. Khandagale, S. K. Patel *et al.*, 2019 Multifaceted activities of DNA polymerase eta: beyond translesion DNA synthesis. Curr. Genet. 65: 649–656. https://doi.org/10.1007/s00294-018-0918-5

Alt, A., K. Lammens, C. Chiocchini, A. Lammens, J. C. Pieck *et al.*, 2007 Bypass of DNA lesions generated during anticancer treatment with cisplatin by DNA polymerase eta. Science 318: 967–970. https://doi.org/10.1126/science.1148242

Bertoletti, F., V. Cea, C. C. Liang, T. Lanati, A. Maffia *et al.*, 2017 Phosphorylation regulates human poleta stability and damage bypass throughout the cell cycle. Nucleic Acids Res. 45: 9441–9454. https://doi.org/10.1093/nar/gkx619

Billon, P., J. Li, J. P. Lambert, Y. Chen, V. Tremblay *et al.*, 2017 Acetylation of PCNA sliding surface by Eco1 promotes genome stability through homologous recombination. Mol. Cell 65: 78–90. https://doi.org/10.1016/j.molcel.2016.10.033

Brands, A., and R. V. Skibbens, 2008 Sister chromatid cohesion role for CDC28-CDK in Saccharomyces cerevisiae. Genetics 180: 7–16. https://doi.org/10.1534/genetics.108.092288

Brown, N. R., M. E. Noble, J. A. Endicott, and L. N. Johnson, 1999 The structural basis for specificity of substrate and recruitment peptides for cyclin-dependent kinases. Nat. Cell Biol. 1: 438–443. https://doi.org/10.1038/15674

Cao, X., C. Li, S. Xiao, Y. Tang, J. Huang *et al.*, 2017 Acetylation promotes TyrRS nuclear translocation to prevent oxidative damage. Proc. Natl. Acad. Sci. USA 114: 687–692. https://doi.org/10.1073/pnas.1608488114

Chan, K. L., M. B. Roig, B. Hu, F. Beckouet, J. Metson *et al.*, 2012 Cohesin's DNA exit gate is distinct from its entrance gate

and is regulated by acetylation. Cell 150: 961–974. https://doi.org/10.1016/j.cell.2012.07.028

Chen, Y. W., J. E. Cleaver, Z. Hatahet, R. E. Honkanen, J. Y. Chang *et al*., 2008 Human DNA polymerase eta activity and translocation is regulated by phosphorylation. Proc. Natl. Acad. Sci. USA 105: 16578–16583. https://doi.org/10.1073/pnas.0808589105

Ciosk, R., M. Shirayama, A. Shevchenko, T. Tanaka, A. Toth *et al*., 2000 Cohesin's binding to chromosomes depends on a separate complex consisting of Scc2 and Scc4 proteins. Mol. Cell 5: 243–254. https://doi.org/10.1016/S1097-2765(00)80420-7

Cipolla, L., F. Bertoletti, A. Maffia, C. C. Liang, A. R. Lehmann *et al*., 2019 UBR5 interacts with the replication fork and protects DNA replication from DNA polymerase eta toxicity. Nucleic Acids Res. 47: 11268–11283. https://doi.org/10.1093/nar/gkz824

Covo, S., J. W. Westmoreland, D. A. Gordenin, and M. A. Resnick, 2010 Cohesin Is limiting for the suppression of DNA damage-induced recombination between homologous chromosomes. PLoS Genet. 6: e1001006. https://doi.org/10.1371/journal.pgen.1001006

Cross, F. R., and K. Levine, 1998 Molecular evolution allows bypass of the requirement for activation loop phosphorylation of the Cdc28 cyclin-dependent kinase. Mol. Cell. Biol. 18: 2923–2931. https://doi.org/10.1128/MCB.18.5.2923

Desany, B. A., A. A. Alcasabas, J. B. Bachant, and S. J. Elledge, 1998 Recovery from DNA replicational stress is the essential function of the S-phase checkpoint pathway. Genes Dev. 12: 2956–2970. https://doi.org/10.1101/gad.12.18.2956

Dorsett, D., and L. Strom, 2012 The ancient and evolving roles of cohesin in gene expression and DNA repair. Curr. Biol. 22: R240–R250. https://doi.org/10.1016/j.cub.2012.02.046

Durando, M., S. Tateishi, and C. Vaziri, 2013 A non-catalytic role of DNA polymerase eta in recruiting Rad18 and promoting PCNA monoubiquitination at stalled replication forks. Nucleic Acids Res. 41: 3079–3093. https://doi.org/10.1093/nar/gkt016

Emsley, P., and K. Cowtan, 2004 Coot: model-building tools for molecular graphics. Acta Crystallogr. D Biol. Crystallogr. 60: 2126–2132. https://doi.org/10.1107/S0907444904019158

Enervald, E., E. Lindgren, Y. Katou, K. Shirahige, and L. Strom, 2013 Importance of Poleta for damage-induced cohesion reveals differential regulation of cohesion establishment at the break site and genome-wide. PLoS Genet. 9: e1003158. https://doi.org/10.1371/journal.pgen.1003158

Enserink, J. M., and R. D. Kolodner, 2010 An overview of Cdk1-controlled targets and processes. Cell Div. 5: 11. https://doi.org/10.1186/1747-1028-5-11

Gerlich, D., B. Koch, F. Dupeux, J. M. Peters, and J. Ellenberg, 2006 Live-cell imaging reveals a stable cohesin-chromatin interaction after but not before DNA replication. Curr. Biol. 16: 1571–1578. https://doi.org/10.1016/j.cub.2006.06.068

Hall, M. C., D. E. Jeong, J. T. Henderson, E. Choi, S. C. Bremmer *et al*., 2008 Cdc28 and Cdc14 control stability of the anaphase-promoting complex inhibitor Acm1. J. Biol. Chem. 283: 10396–10407. https://doi.org/10.1074/jbc.M710011200

Heidinger-Pauli, J. M., E. Unal, and D. Koshland, 2009 Distinct targets of the Eco1 acetyltransferase modulate cohesion in S phase and in response to DNA damage. Mol. Cell 34: 311–321. https://doi.org/10.1016/j.molcel.2009.04.008

Heo, S. J., K. Tatebayashi, and H. Ikeda, 1999 The budding yeast cohesin gene SCC1/MCD1/RHC21 genetically interacts with PKA, CDK and APC. Curr. Genet. 36: 329–338. https://doi.org/10.1007/s002940050507

Ira, G., A. Pellicioli, A. Balijja, X. Wang, S. Fiorani *et al*., 2004 DNA end resection, homologous recombination and DNA damage checkpoint activation require CDK1. Nature 431: 1011–1017. https://doi.org/10.1038/nature02964

Ivanov, D., A. Schleiffer, F. Eisenhaber, K. Mechtler, C. H. Haering *et al*., 2002 Eco1 is a novel acetyltransferase that can acetylate proteins involved in cohesion. Curr. Biol. 12: 323–328. https://doi.org/10.1016/S0960-9822(02)00681-4

Johnson, R. E., C. M. Kondratick, S. Prakash, and L. Prakash, 1999a hRAD30 mutations in the variant form of xeroderma pigmentosum. Science 285: 263–265. https://doi.org/10.1126/science.285.5425.263

Johnson, R. E., S. Prakash, and L. Prakash, 1999b Efficient bypass of a thymine-thymine dimer by yeast DNA polymerase, Poleta. Science 283: 1001–1004. https://doi.org/10.1126/science.283.5404.1001

Kannouche, P., B. C. Broughton, M. Volker, F. Hanaoka, L. H. Mullenders *et al*., 2001 Domain structure, localization, and function of DNA polymerase eta, defective in xeroderma pigmentosum variant cells. Genes Dev. 15: 158–172. https://doi.org/10.1101/gad.187501

Kim, J. S., T. B. Krasieva, V. LaMorte, A. M. Taylor, and K. Yokomori, 2002 Specific recruitment of human cohesin to laser-induced DNA damage. J. Biol. Chem. 277: 45149–45153. https://doi.org/10.1074/jbc.M209123200

Kim, B. J., Y. Li, J. Zhang, Y. Xi, Y. Li *et al*., 2010 Genome-wide reinforcement of cohesin binding at pre-existing cohesin sites in response to ionizing radiation in human cells. J. Biol. Chem. 285: 22784–22792. https://doi.org/10.1074/jbc.M110.134577

Kitazono, A. A., D. A. Garza, and S. J. Kron, 2003 Mutations in the yeast cyclin-dependent kinase Cdc28 reveal a role in the spindle assembly checkpoint. Mol. Genet. Genomics 269: 672–684. https://doi.org/10.1007/s00438-003-0870-y

Krissinel, E., and K. Henrick, 2007 Inference of macromolecular assemblies from crystalline state. J. Mol. Biol. 372: 774–797. https://doi.org/10.1016/j.jmb.2007.05.022

Liebschner, D., P. V. Afonine, M. L. Baker, G. Bunkoczi, V. B. Chen *et al*., 2019 Macromolecular structure determination using X-rays, neutrons and electrons: recent developments in Phenix. Acta Crystallogr. D Struct. Biol. 75: 861–877. https://doi.org/10.1107/S2059798319011471

Lopez-Serra, L., A. Lengronne, V. Borges, G. Kelly, and F. Uhlmann, 2013 Budding yeast Wapl controls sister chromatid cohesion maintenance and chromosome condensation. Curr. Biol. 23: 64–69. https://doi.org/10.1016/j.cub.2012.11.030

Lyons, N. A., and D. O. Morgan, 2011 Cdk1-dependent destruction of Eco1 prevents cohesion establishment after S phase. Mol. Cell 42: 378–389. https://doi.org/10.1016/j.molcel.2011.03.023

Lyons, N. A., B. R. Fonslow, J. K. Diedrich, J. R. Yates, III, and D. O. Morgan, 2013 Sequential primed kinases create a damage-responsive phosphodegron on Eco1. Nat. Struct. Mol. Biol. 20: 194–201. https://doi.org/10.1038/nsmb.2478

Madril, A. C., R. E. Johnson, M. T. Washington, L. Prakash, and S. Prakash, 2001 Fidelity and damage bypass ability of Schizosaccharomyces pombe Eso1 protein, comprised of DNA polymerase eta and sister chromatid cohesion protein Ctf7. J. Biol. Chem. 276: 42857–42862. https://doi.org/10.1074/jbc.M106917200

Masutani, C., R. Kusumoto, A. Yamada, N. Dohmae, M. Yokoi *et al*., 1999 The XPV (xeroderma pigmentosum variant) gene encodes human DNA polymerase eta. Nature 399: 700–704. https://doi.org/10.1038/21447

Michaelis, C., R. Ciosk, and K. Nasmyth, 1997 Cohesin: chromosomal proteins that prevent premature separation of sister chromatids. Cell 91: 35–45. https://doi.org/10.1016/S0092-8674(01)80007-6

Morgan, D. O., 1997 Cyclin-dependent kinases: engines, clocks, and microprocessors. Annu. Rev. Cell Dev. Biol. 13: 261–291. https://doi.org/10.1146/annurev.cellbio.13.1.261

Nagao, K., Y. Adachi, and M. Yanagida, 2004 Separase-mediated cleavage of cohesin at interphase is required for DNA repair. Nature 430: 1044–1048. https://doi.org/10.1038/nature02803

Nasmyth, K., and C. H. Haering, 2009 Cohesin: its roles and mechanisms. Annu. Rev. Genet. 43: 525–558. https://doi.org/10.1146/annurev-genet-102108-134233

Nigg, E. A., 1993 Cellular substrates of p34(cdc2) and its companion cyclin-dependent kinases. Trends Cell Biol. 3: 296–301. https://doi.org/10.1016/0962-8924(93)90011-O

Nooren, I. M., and J. M. Thornton, 2003 Structural characterisation and functional significance of transient protein-protein interactions. J. Mol. Biol. 325: 991–1018. https://doi.org/10.1016/S0022-2836(02)01281-0

Peddu, C., S. Zhang, H. Zhao, A. Wong, E. Y. C. Lee *et al.*, 2018 Phosphorylation alters the properties of Pol eta: implications for translesion synthesis. iScience 6: 52–67. https://doi.org/10.1016/j.isci.2018.07.009

Peters, J. M., and T. Nishiyama, 2012 Sister chromatid cohesion. Cold Spring Harb. Perspect. Biol. 4: a011130.

Plachta, M., A. Halas, J. McIntyre, and E. Sledziewska-Gojska, 2015 The steady-state level and stability of TLS polymerase eta are cell cycle dependent in the yeast S. cerevisiae. DNA Repair (Amst.) 29: 147–153. https://doi.org/10.1016/j.dnarep.2015.02.015

Powers, K. T., A. H. Elcock, and M. T. Washington, 2018 The C-terminal region of translesion synthesis DNA polymerase eta is partially unstructured and has high conformational flexibility. Nucleic Acids Res. 46: 2107–2120. https://doi.org/10.1093/nar/gky031

Rolef Ben-Shahar, T., S. Heeger, C. Lehane, P. East, H. Flynn *et al.*, 2008 Eco1-dependent cohesin acetylation during establishment of sister chromatid cohesion. Science 321: 563–566. https://doi.org/10.1126/science.1157774

Rowland, B. D., M. B. Roig, T. Nishino, A. Kurze, P. Uluocak *et al.*, 2009 Building sister chromatid cohesion: smc3 acetylation counteracts an antiestablishment activity. Mol. Cell 33: 763–774. https://doi.org/10.1016/j.molcel.2009.02.028

Ström, L., H. B. Lindroos, K. Shirahige, and C. Sjogren, 2004 Postreplicative recruitment of cohesin to double-strand breaks is required for DNA repair. Mol. Cell 16: 1003–1015. https://doi.org/10.1016/j.molcel.2004.11.026

Ström, L., C. Karlsson, H. B. Lindroos, S. Wedahl, Y. Katou *et al.*, 2007 Postreplicative formation of cohesion is required for repair and induced by a single DNA break. Science 317: 242–245. https://doi.org/10.1126/science.1140649

Toulmay, A., and R. Schneiter, 2006 A two-step method for the introduction of single or multiple defined point mutations into the genome of Saccharomyces cerevisiae. Yeast 23: 825–831. https://doi.org/10.1002/yea.1397

Ubersax, J. A., E. L. Woodbury, P. N. Quang, M. Paraz, J. D. Blethrow *et al.*, 2003 Targets of the cyclin-dependent kinase Cdk1. Nature 425: 859–864. https://doi.org/10.1038/nature02062

Uhlmann, F., 2016 SMC complexes: from DNA to chromosomes. Nat. Rev. Mol. Cell Biol. 17: 399–412. https://doi.org/10.1038/nrm.2016.30

Unal, E., A. Arbel-Eden, U. Sattler, R. Shroff, M. Lichten *et al.*, 2004 DNA damage response pathway uses histone modification to assemble a double-strand break-specific cohesin domain. Mol. Cell 16: 991–1002. https://doi.org/10.1016/j.molcel.2004.11.027

Unal, E., J. M. Heidinger-Pauli, and D. Koshland, 2007 DNA double-strand breaks trigger genome-wide sister-chromatid cohesion through Eco1 (Ctf7). Science 317: 245–248 (erratum: Science 318: 1722). https://doi.org/10.1126/science.1140637

Unal, E., J. M. Heidinger-Pauli, W. Kim, V. Guacci, I. Onn *et al.*, 2008 A molecular determinant for the establishment of sister chromatid cohesion. Science 321: 566–569. https://doi.org/10.1126/science.1157880

Waterhouse, A., M. Bertoni, S. Bienert, G. Studer, G. Tauriello *et al.*, 2018 SWISS-MODEL: homology modelling of protein structures and complexes. Nucleic Acids Res. 46: W296–W303. https://doi.org/10.1093/nar/gky427

Waters, L. S., B. K. Minesinger, M. E. Wiltrout, S. D'Souza, R. V. Woodruff *et al.*, 2009 Eukaryotic translesion polymerases and their roles and regulation in DNA damage tolerance. Microbiol. Mol. Biol. Rev. 73: 134–154. https://doi.org/10.1128/MMBR.00034-08

Zhang, J., X. Shi, Y. Li, B. J. Kim, J. Jia *et al.*, 2008 Acetylation of Smc3 by Eco1 is required for S phase sister chromatid cohesion in both human and yeast. Mol. Cell 31: 143–151. https://doi.org/10.1016/j.molcel.2008.06.006

Communicating Editor: J. Nickoloff